J. Phys. II France 6 (1996) 1781–1795 DECEMBER 1996, PAGE 1781

Dilute Solutions of Diblock Copolymers in a Selective Solvent: I. Evidence for Spherical Star like Micelles

M. Adam ([1,*]), J.-P. Carton ([2]), S. Corona-Vallet ([1]) and D. Lairez ([1])

([1]) Laboratoire Léon Brillouin, CEA-CNRS, CEA Saclay, 91191 Gif-sur-Yvette Cedex, France
([2]) Service de Physique de l'État Condensé, CEA Saclay, 91191 Gif-sur-Yvette Cedex, France

(Received 16 April 1996, received in final form 29 August 1996, accepted 2 September 1996)

PACS.61.25.Hq – Macromolecular and polymer solutions; polymer melts; swelling
PACS.61.41.+e – Polymers, elastomers, and plastics
PACS.82.70.Dd – Colloids

Abstract. — Diblock copolymer polystyrene-polyisoprene PS-PI is studied in dilute solution at room temperature in methylcyclohexane, a good solvent for polyisoprene and a theta solvent for polystyrene at $T_\theta = 70$ °C. The molecular mass of the copolymer is 1.1×10^6 g/mol and the polystyrene weight fraction is 36%. The diblock copolymer aggregates into star like micelles which are studied by static and quasielastic light scattering. Both techniques lead to a full characterization of the micelles. Well below the overlap concentration, the data are strongly dependent on micelle interactions. The scattered intensity (the diffusion coefficient) presents a maximum (a minimum) at a scattering vector which is concentration dependent. From this dependence we infer that the micelles are in a liquid phase, the mean distance between first neighbor being 400 nm at a concentration $C = 10^{-3}$ g/cm^3. From these measurements we can deduce the mobility per monomer and demonstrate that the micelles move in an effective medium having the macroscopic viscosity of the solution.

Introduction

Block copolymers are made of several sequences belonging to different chemical species. In the bulk, polymer incompatibility is responsible for the existence of a wide range of structures. In a selective solvent, *i.e.* a bad solvent for one of the species, A, and a good solvent for the other, B, polymer-solvent interaction dominates. In this case, the interfacial energy between the A blocks and the solvent acts as a driving force for aggregation of the copolymers. In order to describe theoretically the thermodynamics of this aggregation process, one has to take into account all the terms which equilibrate this driving force, such as the translation entropy loss and also those which are linked to the aggregate geometry. For instance, spherical copolymer micelles are often described using a model of star like polymers [1]. This model introduces an osmotic energy term due to the polymer concentration inside the corona which is made of the block in good solvent condition; however, in some cases, additional terms such as the conformational entropy of copolymer chains in the micelle have to be taken into consideration. For example, telechelic triblock copolymers need a backfolding of their middle block to form

(*) Author for correspondence (e-mail: adam@ill.fr)

spherical and flower like micelles. The corresponding entropy loss prevents the copolymer from forming this kind of micelles as the solvent selectivity is comparatively insufficient [2,3].

The case of diblock copolymers is expected to be simpler from a theoretical point of view and is extensively studied [4,5]. Usually, experimentalists choose to be in a non solvent condition for the A block and to determine the different parameters characterizing the micelles using different diblock copolymers. Here we choose to investigate the behavior of a diblock copolymer below the theta temperature of one block. This allows us to tune the solvent selectivity by varying the temperature and to relate macrophase separation to microphase separation (aggregation). The results obtained are not as simple as expected and the phase diagram is quite complex (see Fig. 1). Consequently, the presentation of this work is divided in two parts and this first paper is only concerned with the micelles obtained at low temperature (regime III in Fig. 1). In this regime, experimental evidence for spherical and star like micelles is discussed. This will help us to understand the phase diagram and the different structures obtained.

1. Sample Characteristics and Experimental Devices

This paper presents experimental results obtained on a diblock copolymer polystyrene-polyisoprene (PS-PI) in dilute solution. The diblock copolymer PS-PI was synthesized and characterized by PSS (Mainz Germany): total molecular weight $M_w = 1.1 \times 10^6$ g/mol, polystyrene weight fraction $w_{PS} = 0.36$, polydispersity index $I_p = 1.08$. The solvent used is methylcyclohexane, a good solvent for polyisoprene at all temperatures and a theta solvent for polystyrene at $T_\theta = 70$ °C. The methylcyclohexane is kept under molecular sieves to prevent water absorption. The polymer solutions prepared by weighing were placed in sealed cells and kept at room temperature.

Details of the home made light scattering apparatus as well as the data treatment have been fully described elsewhere [6]. The argon laser (wavelength $\lambda = 488$ nm) is focused in the sample cell which is placed in a vessel containing toluene and surrounded by a copper cylinder (high thermal conductivity). The base of the cylinder is in contact with a copper box in which thermostated water flows. A radial slit on the copper cylinder allows light scattering experiments to be performed at scattering angles θ ranging from 10° to 150°. The vertical thermal gradient measured at the center of the sample is less than 0.2 °C/cm.

2. Measured Quantities: Theoretical Background

2.1. Static Light Scattering. — Let us call I the intensity scattered by the polymer normalized by the intensity scattered by the solvent under the same experimental conditions, then:

$$\frac{I(q)}{K \times C} = C\frac{kT}{E(q)} \tag{1}$$

where k is the Boltzmann constant, T the absolute temperature, K the apparatus constant and q the scattering vector. They are defined by $q = \frac{4\pi}{\lambda} n \times \sin(\theta/2)$, and $K = (4\pi^2 n^2)(\mathrm{d}n/\mathrm{d}C)^2/(\lambda^4 N_a \mathcal{R})$, n is the refractive index, N_a the Avogadro's number, $\mathcal{R}$ the solvent Rayleigh ratio and $\mathrm{d}n/\mathrm{d}C$ the contrast between polymer and solvent. In equation (1), $E(q)$ is the q dependent longitudinal elastic modulus of the solution [7]. For liquid polymer solutions, only the bulk osmotic contribution is relevant for static measurements: $E(q) = C\mathrm{d}\pi(q)/\mathrm{d}C$. Far below the overlap concentration C^*, it can be written using a virial expansion of the osmotic pressure π:

$$E(q) = \frac{kTC}{M(q)}(1 + 2M(q)A_2(q)C + \ldots) \tag{2}$$

$M(q)$ is the molecular mass accounting for the form factor $P(q)$ of molecules: $M(q) = M \times P(q)$, and A_2 the second virial coefficient reflecting the two body interaction term. The behavior of mass, form factor and second virial coefficient will now be discussed in the framework of the Daoud-Cotton model [8] for star like polymers, a model usually [1] used to describe spherical copolymer micelles. In this model, due to the fact that the f arms of the star are constrained to reach a unique point (the center of the star), thermodynamic interactions are screened for length scales smaller than the size of the overall polymer. These arms form an assembly of blobs whose sizes increase with the distance from the center of the polymer. The largest blobs have a size $\xi = R_g f^{-1/2}$. At very low concentration ($C \ll C^*$), the shape of the scattered intensity per monomer is theoretically predicted [9] and experimentally verified [10]. At length scales q^{-1} larger than the radius of gyration R_g of the polymers, the scattered intensity is sensitive to the mass of the polymer and decreases linearly with q^2, allowing the determination of R_g: $I(q)/(K \times C) = f M_a(1 - q^2 R_g^2/3)$. The radius of gyration R_g and the mass of one arm, M_a, are linked by:

$$R_g = M_a^{1/D} f^{0.2} \tag{3}$$

where D is the fractal dimension. For $q\xi > 1$, one recovers the q^{-D} dependence of the scattered intensity found for linear polymer. In this q range the scattered intensity per monomer is expected to be independent of the number of arms and equal to the intensity scattered by linear polymers. For $1/R_g < q < 1/\xi$, a fortuitous q^{-3} dependence of the form factor is predicted. In this regime, the scattered intensity $I(q)/C$ remains dependent on the number of arms ($f^{0.4}$).

Near the overlap concentration C^*, due to their high internal concentration compared to the macroscopic concentration, star polymers do not interpenetrate [11]. Therefore, upon increasing the concentration, the star polymer solution shifts from a gas like to a liquid like state. In this concentration regime a virial expansion cannot account for the structure factor. The scattered intensity presents a maximum at $q^\dagger$, which corresponds to a first neighbor mean distance rather than a long range order. This characteristic scattering vector value $q^\dagger$ depends on the concentration as:

$$q^\dagger = \frac{\pi}{R_g} \left(\frac{C}{C^*} \right)^{1/3} \tag{4}$$

As the concentration increases above C^*, *i.e.* as the macroscopic osmotic pressure becomes larger than the osmotic pressure inside the star, polymers interpenetrate each other. The intensity scattered by a semi-dilute solution of star polymers is thus identical to that of linear polymers [12]. The system does not crystallize [13].

In the case of block copolymers, the contrast difference between the two blocks implies that an apparent radius of gyration, R_{gapp}, can only be measured by scattering experiments (a limiting case would be one where one block is invisible). This problem is relevant for light scattering [14] as well as for neutron scattering experiments [15]. In the case of block copolymers the refractive index increment dn/dC is the sum of the contribution of each block weighted by its weight fraction [16] ($w_i = M_i/M$) : $\langle dn/dC \rangle = w_{PS}(dn/dC)_{PS} + w_{PI}(dn/dC)_{PI}$. One has:

$$R_{gapp}^2 = \alpha_{PS} R_{gPS}^2 + \alpha_{PI} R_{gPI}^2 + \alpha_{PS}\alpha_{PI} G_{PS-PI}^2 \tag{5}$$

where $\alpha_i = w_i(dn/dC)_i/\langle dn/dC \rangle$ and G_{PS-PI} is the distance between center of gravity of the two species. This distance depends on the copolymer conformation. The two situations for which G_{PS-PI} can be easily calculated are a Gaussian ($G_{PS-PI}^2/R_g^2 = 2$) and a concentric ($G_{PS-PI}^2 = 0$) distribution of the two species. The former case applied to the unimer of the diblock PS-PI studied here (in our case: $\alpha_{PS} \cong \alpha_{PI} = 0.5$) leads to $R_{gapp}^2 = R_g^2$. Note that taking into account excluded volume effects leads to a ratio $G_{PS-PI}^2/R_g^2 = 2.20 \pm 0.02$ but this

does not result in a significant difference between R_{gapp} and R_g. The latter case corresponds to micelles made of a dense core of PS and a fractal (star like) corona of PI. For the dense and spherical core, the ratio of the radius of gyration, R_{gPS}, to the overall radius of the core, R_{core}, is given by:

$$\frac{R_{gPS}^2}{R_{core}^2} = \frac{3}{5} \tag{6}$$

while for the fractal corona, the ratio of the radius of gyration, R_{gPI}, to the overall radius of the corona, R_t, is given by:

$$\frac{R_{gPI}^2}{R_t^2} = \frac{D}{D+2}\frac{1-\Delta^{D+2}}{1-\Delta^D} \tag{7}$$

where D is the fractal dimension on the star like corona and Δ the ratio of the internal to the external radius of the corona, *i.e.* the ratio of the radius of the core to the overall radius of the micelle: $\Delta = R_{core}/R_t$. Using equations (6) and (7) one obtains for the apparent radius of gyration:

$$R_{gapp}^2 = R_t^2\left(\frac{3}{5}\alpha_{PS}\Delta^2 + \alpha_{PI}\frac{D}{D+2}\frac{1-\Delta^{D+2}}{1-\Delta^D}\right) \tag{8}$$

In the case of the diblock studied here, assuming a Gaussian conformation for both blocks $\Delta = 0.60$ leads to $R_t/R_{gapp} = 1.6$. This value corresponds to the lower bound of R_t/R_{gapp} which increases for increasing association number due to the stretching of the PI (decrease of Δ).

2.2. Quasielastic Light Scattering. — Quasielastic light scattering experiments are performed in the homodyne mode. The time dependence of the dynamic structure factor is an exponential decay, whose characteristic time τ, measured at a given scattering vector q, leads to a diffusion coefficient $\mathcal{D}(q)$:

$$\mathcal{D}(q) = \frac{1}{\tau q^2} \tag{9}$$

In general, the diffusion coefficient is the product of the mobility $\mu(q)$ per monomer and the elastic modulus $E(q)$ which tends to restore the uniform concentration after a fluctuation [17, 18]. Note that $\mu(q)$ is the mobility of the diffusing object divided by its mass and corresponds to the inverse of the sedimentation coefficient. As already explained for liquid polymer solutions the only restoring force is the osmotic bulk modulus $E(q) = C\mathrm{d}\pi(q)/\mathrm{d}C$:

$$\mathcal{D}(q) = \frac{\mu(q)E(q)}{C} \tag{10}$$

Thus, using equation (1) one obtains, for the q dependent mobility per monomer:

$$\frac{I(q)}{K \times C} \times \mathcal{D}(q) = kT \times \mu(q) \tag{11}$$

K being the apparatus constant.

To illustrate equations (10) or (11) let us first examine the zero concentration and zero scattering vector limiting cases. The mobility is the ratio of the mass of the object to the friction it undergoes. In the Zimm model, hydrodynamic interactions between monomers imply that the polymer coil motion is equivalent to that of a sphere:

$$\mu_{(q\to 0, C\to 0)} = \frac{M}{6\pi\eta_0 R_H} \tag{12}$$

where η_0 is the solvent viscosity and R_H the hydrodynamic radius. The scattered intensity per monomer being proportional to the mass M, one recovers the well-known result (Stokes-Einstein relation) for the diffusion coefficient $\mathcal{D}_{(q\to 0,C\to 0)} = kT/(6\pi\eta_0 R_H)$. The hydrodynamic radius thus defined is proportional to the radius of gyration: $R_H/R_g = \sqrt{5/3}$ for dense spheres, $R_H/R_g = 0.64$ and 0.80 for excluded volume [19] and Gaussian polymer chains, respectively.

At finite concentration, interactions have to be taken into account. A virial expansion of the osmotic modulus accounts for thermodynamic interactions (see Eq. (2)). As for hydrodynamic interactions, a concentration expansion is used to account for the increase in viscosity encountered by the diffusing particle:

$$\eta = \eta_0(1 + [\eta]C + k_H([\eta]C)^2 + . \quad) \tag{13}$$

where $[\eta]$ is the intrinsic viscosity and k_H the Huggins constant. One obtains for the mobility per monomer:

$$\mu_{(q\to 0)} = \frac{kTM}{6\pi\eta_0 R_H}(1 - [\eta]C + . \quad) \tag{14}$$

and

$$\mathcal{D}_{(q\to 0)} = \frac{kT}{6\pi\eta_0 R_H}(1 + (2MA_2 - [\eta])C + . \quad) \tag{15}$$

Note that such interpretation of the concentration dependence of the diffusion coefficient assumes that the actual form and size of the polymers are not affected by the concentration.

Let us consider the q dependence of these quantities. In dilute solutions of linear polymers at $qR_g > 1$, both static and dynamic experiments are sensitive to concentration fluctuations at a length scale q^{-1} The scattered intensity is proportional to the mass $M(q)$ *i.e.* the number of monomers in a volume q^{-3} which scatter coherently: $M(q) \propto q^{-D}$ As for the hydrodynamic length, for the same reason it is proportional to q^{-1}, in other words, only part of the polymer of size q^{-1} is viewed to move cooperatively [18]:

$$\mu_{(qR_g>1)} = \frac{M(q)}{6\pi\eta_0 q^{-1}} \tag{16}$$

Thus, at these length scales, one obtains a q dependent diffusion coefficient:

$$\mathcal{D}_{(qR_g>1)} = \frac{kT}{6\pi\eta_0} q \tag{17}$$

which is characteristic of internal modes in the Zimm model for polymer dynamics. In the Rouse model, which does not consider hydrodynamic interactions between monomers, the friction undergone by the polymer is the sum of the friction of each monomer. Internal modes thus correspond to a diffusion coefficient $\mathcal{D}_{(qR_g>1)}$ proportional to q^2. This can be only observed if one polymer is visible among the others. In the case of star like polymers, the blob model applies to hydrodynamic interactions. At distance q^{-1} larger than ξ there is no correlation between fluctuations [20]. Thus, even at length scales q^{-1} between R_g and ξ, the concentration fluctuations relax through translation of the whole star polymer. This leads to a q independent diffusion coefficient. One has to keep in mind the q^{-3} dependence of the scattered intensity in this regime. For $q\xi > 1$, one recovers a q dependent diffusion coefficient as for linear polymers.

As for linear polymers, the mobility per monomer is sensitive to concentration only through the viscosity. In addition, this viscosity is a decrease monotonously with the scattering vector q: η is equal to the macroscopic viscosity at $q \to 0$, while η corresponds to the solvent viscosity at $q\xi > 1$. Thus as the concentration is increased near the overlap concentration C^*, due to

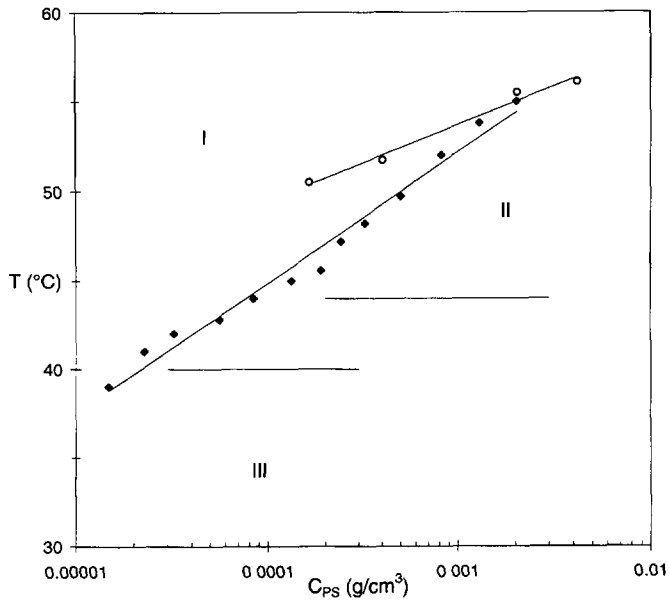

Fig. 1. — Critical aggregation temperature (CAT, full symbols) of copolymer PS-PI and demixion temperature (DT, empty symbols) of homopolymer PS precursor in methylcyclohexane (T_θ = 70 °C) as a function of the logarithm of the polystyrene concentration ($C_{PS} = w_{PS} \times C$). Straight lines are guides for the eyes. At $T >$ CAT (I), only free copolymers are present. For $T <$ 40 °C $<$ CAT (III), copolymers form star like micelles. For 44 °C $< T <$ CAT (II), the aggregates formed are large, with a small degree of association and a low density structure.

the fact that the scattered intensity $I(q)$ presents a maximum at a scattering vector $q^\dagger$, one expects that the diffusion coefficient shows a minimum at the same q value. This minimum of the diffusion coefficient can be interpreted as a diffusion hindrance of one star polymer by its neighbors which are at a distance $d = 2\pi/q^\dagger$.

3. Experimental Results

3.1. Phase Diagram. — In part 2, what is expected for the aggregation process considered as a microphase separation will be detailed from a theoretical point of view. The expected laws governing the growth of the aggregates as the temperature is decreased from the theta point of the A block (PS), will be given. In this paper, only the phase diagram will be presented. Copolymer aggregation occurs at a critical aggregation temperature (CAT) which depends strongly on the concentration. In methylcyclohexane, the CAT is measured as follows: the sample is brought to high temperature (55 °C), after stabilization of the scattered intensity at a fixed scattering angle (usually $\theta = 20°$) the temperature is decreased by 1 °C steps. Once the intensity increases by a factor of 2, the temperature is increased by 1/2 degree steps. The CAT, independent of the thermal path, corresponds to the temperature at which the intensity just begins to increase. In Figure 1 the CAT is plotted as a function of the polystyrene concentration [21] ($C_{PS} = w_{PS} \times C$) and is compared to the demixion temperature DT of the homopolymer polystyrene precursor ($M_{PS} = 4 \times 10^5$ g/mol). The demixion temperature DT is measured by decreasing the temperature from $T >$ DT. It corresponds to the temperature at which the

scattered intensity diverges. In this representation, the two curves CAT and DT coincide at high concentrations ($C_{PS} > 10^{-3}$ g/cm^3) but differ significantly at low concentrations. This experimental result will be discussed in part 2.

Figure 1 is divided into several domains corresponding to different structures for the copolymer aggregates. At temperatures higher than the CAT, only free copolymers are present (regime I), they will be called unimers in the following [5]. For $T < 40$ °C $<$ CAT (regime III), copolymers are associated in star like micelles. For 44 °C $< T <$ CAT, (regime II) the aggregates formed are large, with a small degree of association and a low density structure. This paper is only concerned with the characterization of the unimers (regime I, experiments performed at CAT $< T = 56$ °C) and the star like micelles (regime III). Concentration effects are studied at room temperature on samples which were quenched from $T = 60$ °C (oven) to $T = 15$ °C (water bath).

3.2. Characterization of Diblock Copolymers. — The characterization of unimers was performed at $T = 56$ °C. The inverse of the scattered intensity extrapolated to zero q and zero concentration is equal to: $C/I_{q\to 0} = (3.47 \pm 0.1) \times 10^{-5}$ g/cm^3. Knowing the constant $K = 2.39 \times 10^{-2}$ cm^{3}g^{-2}mol, the measured intensity corresponds to a molecular weight of $(1.20 \pm 0.06) \times 10^6$ g/mol, in good agreement with the value given by the supplier. The concentration dependence of the zero q scattered intensity allows us to determine the second virial coefficient: $MA_2 = 450$ cm^3/g. The apparent radius of gyration deduced from the q dependence of the scattered intensity measured at each concentration and extrapolated to zero concentration is equal to $R_{gapp} = 64 \pm 3$ nm. The diffusion coefficient measured by quasi elastic light scattering is found to be independent of the scattering vector q but depends on the concentration: $\mathcal{D}_{(C\to 0)} = (18.5 \pm 0.5) \times 10^{-8}$ cm^2/s. Using the solvent viscosity $\eta_{0(T=56\ °C)} = 4.46 \times 10^{-3}$ P, the hydrodynamic radius is found to be equal to $R_H = 29.5 \pm 1$ nm. These values lead to a ratio R_H/R_{gapp} equal to 0.46 instead of 0.64 or 0.8 for homopolymer in good or theta solvent, respectively. This indicates that unimers do not adopt the same conformation as homopolymers, because as seen previously in our case ($\alpha_{PS} \cong \alpha_{PI}$) the actual radius of gyration should be equal to R_{gapp}. This could be an indication that the distance between centers of gravity of the two species is larger than in the Gaussian case due to repulsion between the two blocks.

3.3. Spherical Star Like Micelles. — Decreasing the temperature to below 40 °C increases the values of measured quantities such as the radius of gyration, the hydrodynamic radius as well as the scattered intensity per monomer. This is attributed to copolymer micellization and will be detailed in part 2. Let us focus on measurements performed at room temperature on quenched micelles. Samples having concentration ranging from 3.3×10^{-5} to 4.8×10^{-3} g/cm^3 were rapidly transferred from an oven (60 °C) to a water bath (15 °C).

3.3.1. Static Light Scattering. — In Figure 2, the apparent molecular weight deduced from the scattered intensity per monomer ($M_{app}(q) \simeq I(q)/(K \times C) = M \times P(q) \times (1 - 2MA_2C)$) is plotted as a function of the reduced scattering vector qR_{gapp} for the 3 lowest concentrations ($1.7 \times 10^{-5} < C$ (g/cm^3) $< 5 \times 10^{-5}$). The apparent radius of gyration $R_{gapp} = 68 \pm 3$ nm is deduced from extrapolation to zero concentration. The highest value of qR_{gapp} accessible by light scattering ($qR_{gapp\ max} = 2.4$) does not allow us to obtain any direct information on the internal structure of the micelles. For $qR_{gapp} > 1.5$, the variation of the scattered intensity is of the order of $q^{-0.8}$; the exponent is even smaller than the value of 1.7 found for linear polymers. The apparent molecular weight decreases as the concentration increases indicating a positive second virial coefficient, *i.e.* repulsive interactions between micelles. The molecular mass

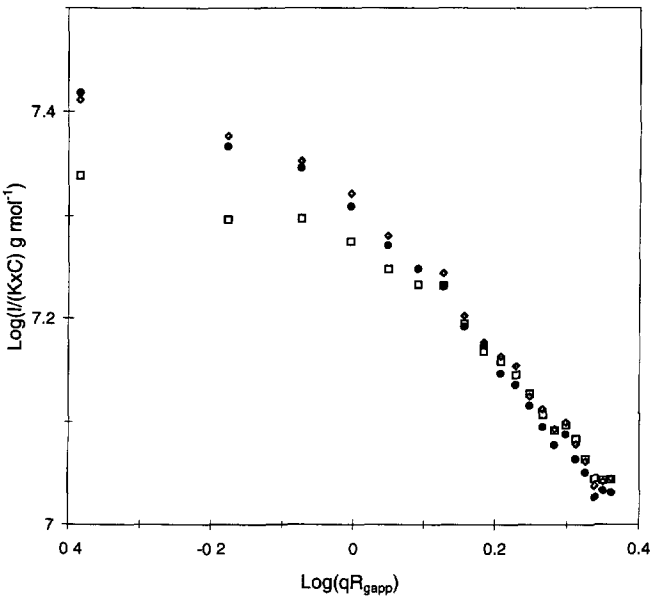

Fig. 2. — Logarithm of the light scattered intensity per monomer $I(q)/(KC) = M \times P(q)$ as a function of the logarithm of the reduced scattering vector qR_{gapp}, where R_{gapp} is the apparent radius of gyration measured for the 3 lowest concentrations: C (g/cm^3) $= 4.9 \times 10^{-5}$, 3.3×10^{-5}, 1.7×10^{-5} (empty, gray and black symbols, respectively). The association number p deduced from the zero q scattering vector limit is equal to 20 ± 1.

$M = (2.4 \pm 0.1) \times 10^7$ g/mol obtained from extrapolation to zero concentration corresponds to $p = 20 \pm 1$ for the association number.

For concentrations higher than 4.6×10^{-4} g/cm^3, the q dependent scattered intensity presents a maximum at $q^\dagger$ (see Fig. 3) as expected for star like polymers. In Figure 3, one can see that, for $q > q^\dagger$ all the curves coincide within 5%. This behavior is a first indication of a constant association number, irrespective of the concentration. In Figure 4, the position $q^\dagger$ of the maximum is plotted as a function of the concentration. As expected for a three dimensional packing of spheres, a $C^{1/3}$ law is found:

$$\frac{q^\dagger}{C^{1/3}} = 0.160 \pm 0.005 \tag{18}$$

where C is expressed in g/cm^3 and q in nm^{-1} This result yields a corresponding mean distance between two neighboring micelles, $d = 2\pi/q^\dagger$, and thus the volume per micelle. The product of this volume to the macroscopic concentration would provide another way to deduce the micelle association number. One obtains, irrespective of the concentration:

$$p = \frac{\frac{\pi d^3}{6} C \times N_{\mathrm{a}}}{M} = 17 \pm 2 \tag{19}$$

in good agreement with the value determined from the molecular weight measurement.

3.3.2. q Dependence of the Diffusion Coefficient. — Quasielastic light scattering measurements were also performed on the above samples. For the experiments reported here, the time dependent dynamic structure factor is a single exponential decay, at all scattering vectors and

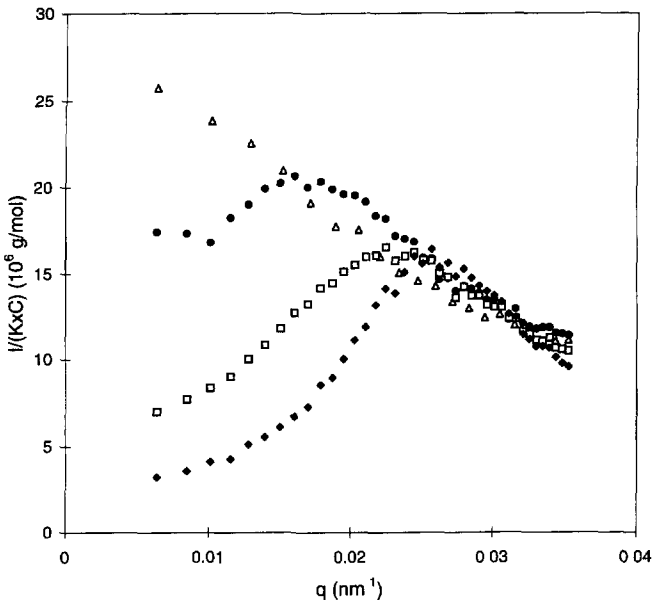

Fig. 3. — Light scattered intensity per monomer $I(q)/(KC)$ as a function of the scattering vector q. Only some of the studied samples are represented C (g/cm^3) = 4.8×10^{-3}, 3.0×10^{-3}, 1.1×10^{-3}, 3.3×10^{-5} for diamonds, squares, circles and triangles symbols, respectively. For the 3 highest concentrations, a scattered intensity maximum is observed.

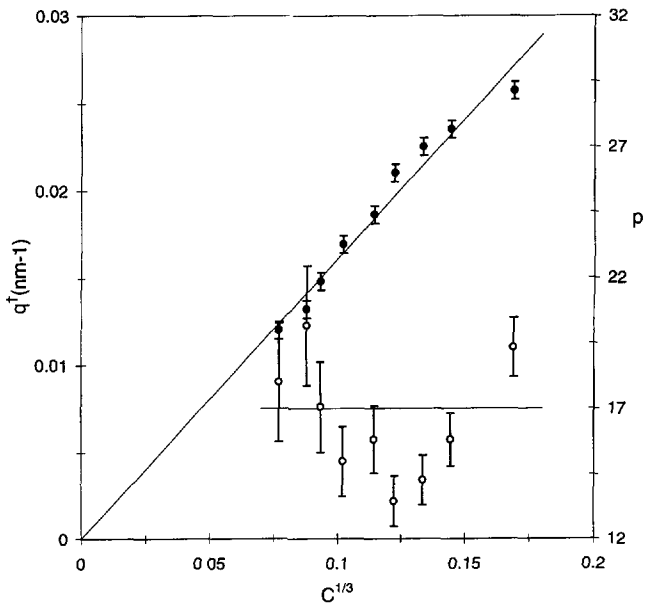

Fig. 4. — Scattering vector position, $q^\dagger$, (full symbols) of the maximum of light scattered intensity as a function $C^{1/3}$ The linear behavior of $q^\dagger = (0.160 \pm 0.005) \times C^{1/3}$ allows us to deduce the association number (empty symbols) from the corresponding mean distance between two neighboring micelles $d = 2\pi/q^\dagger \cdot p = (\pi d^3/6)C \times N_a/M$. The mean value for p is equal to 17 ± 2.

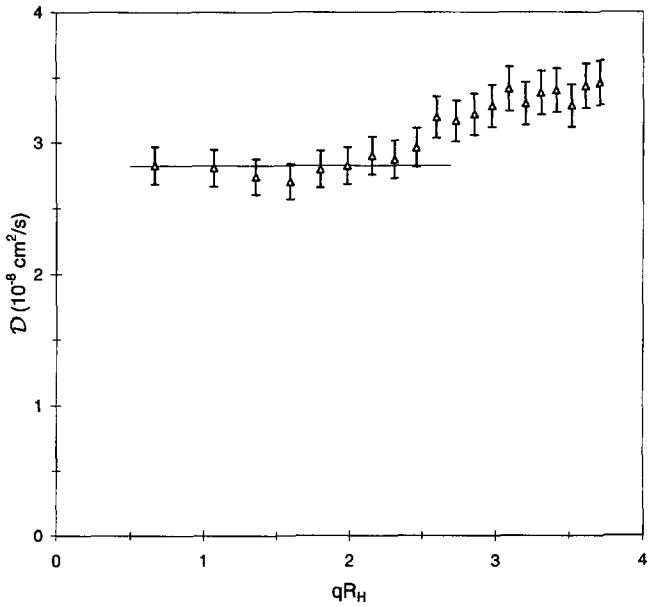

Fig. 5. — Diffusion coefficient $\mathcal{D}$ measured at a concentration $C = 3.3 \times 10^{-5}$ g/cm^3, as a function of the reduced scattering vector qR_H, where R_H is the hydrodynamic radius of the micelle. The independence of $\mathcal{D}$ with the reduced scattering vector qR_H for $qR_H \leq 2.5$ is an experimental evidence for the star like micelle structure. The straight line corresponds to the mean value obtained at low q: $\mathcal{D} = (2.82 \pm 0.05) \times 10^{-8}$ cm^2/s from which R_H is deduced (see text for high q behavior).

concentrations studied. In fact, for the highest concentration, the non exponentiality is so small that no physics can be extracted from it.

In Figure 5, the diffusion coefficient measured for the lowest concentration ($C = 3.3 \times 10^{-5}$ g/cm^3) is plotted as a function of qR_H. The hydrodynamic radius R_H is deduced from the diffusion coefficient measured at small q: $\mathcal{D} = (2.82 \pm 0.05) \times 10^{-8}$ cm^2/s. From the Stokes-Einstein relation and the solvent viscosity ($\eta_{0(T=20\ ^\circ C)} = 7.25 \times 10^{-3}$ P), one obtains $R_H = (106 \pm 2)$ nm. Note that due to the contrast difference between the 2 species, the radius of gyration is apparent while interactions, and thus the hydrodynamic radius, refer to the overall size of the micelles (see Sect. 3.3.3). The diffusion coefficient shows a slight increase with scattering vector for $qR_H > 2.5$ (see Fig. 5). In fact, the highest value of $q = 3.5 \times 10^{-2}$ nm^{-1} corresponds to $q\xi = 0.82$ with $\xi = R_H/\sqrt{P} = 24$ nm; in this case dynamic measurements could begin to be sensitive to internal modes.

The hydrodynamic radius thus determined allows the overlap concentration C^* of the micelles, *i.e.* their internal concentration, to be calculated: $C^* = M/(N_a 4/3 \times \pi R_H^3)$. One gets $C^* = 7 \times 10^{-3}$ g/cm^3. This estimation allows us to express the concentration range investigated in this paper in term of the ratio C/C^*:

$$2 \times 10^{-3} < C/C^* < 0.6 \tag{20}$$

Note that the scattered intensity peak described in Section 3.3.1 appears at C/C^* of the order of 0.05.

In Figure 6, the diffusion coefficient extrapolated to zero scattering vector $\mathcal{D}_{(q \to 0)}$, is plotted as a function of the concentration. In the whole concentration range, the diffusion coefficient is independent of the concentration: for $1.7 \times 10^{-5} < C$ (g/cm^3) $< 4.8 \times 10^{-3}$, $\mathcal{D}_{(q \to 0)} =$

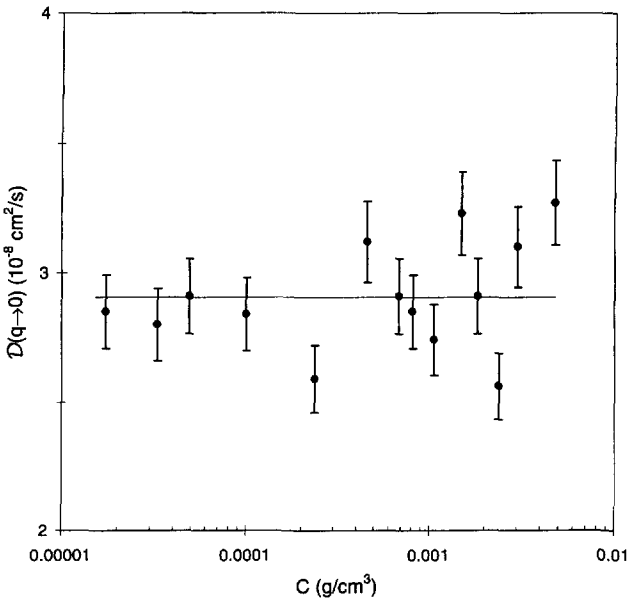

Fig. 6. — The zero scattering vector limit of the diffusion coefficient $\mathcal{D}_{(q\to 0)}$ as a function of the concentration. No concentration dependence is observed, the mean value (straight line) being $\mathcal{D}_{(q\to 0)} = (2.9 \pm 0.2) \times 10^{-8}$ cm^2/s.

$(2.9\pm 0.2)\times 10^{-8}$ cm^2/s in agreement with the value reported for the lowest concentration. The concentration independence of the diffusion coefficient $\mathcal{D}_{(q\to 0)}$, indicates that thermodynamic interactions counterbalance hydrodynamic interactions (see Eq. (15)).

As the concentration increases, the diffusion coefficient becomes dependent on the scattering vector q (see Fig. 7) and presents a minimum at a value q^* which is concentration dependent. For $q \to 0$ all the curves merge, while for $q/q^* > 1$, the diffusion coefficient decreases with concentration. This feature will be discussed below.

3.3.3. Mobility. — At each scattering angle, for each concentration, both the scattered intensity and the diffusion coefficient were measured. As mentioned above, the product of these two quantities leads to the mobility per monomer. In Figure 8, the mobility per monomer is plotted as a function of the scattering vector q. The most noticeable result is the disappearance of the singularity of the curves which are monotone, in other words $q^\dagger = q^*$, the scattered intensity maximum being well compensated by the diffusion coefficient minimum. This result indicates that thermodynamic and hydrodynamic interactions are sensitive to the same length scale, *i.e.* the overall size of micelles.

The mobility per monomer is the ratio of a q dependent mass (form factor) and a friction which is also q dependent *via* the viscosity. In fact, for the zero scattering vector limit, the friction is related to the macroscopic viscosity of the solution, while at $q\xi > 1$ it is related to the solvent viscosity. In Figure 8, one can see that the mobility is strongly concentration dependent at low q, but this dependence decreases at high q, in agreement with a concentration and q dependent viscosity. For the lowest concentration here studied ($C = 3.3 \times 10^{-5}$ g/cm^3) the macroscopic viscosity being the solvent viscosity, the q dependence of the mobility only reflects the micelle form factor. This q dependence is compensated by the q dependence of the

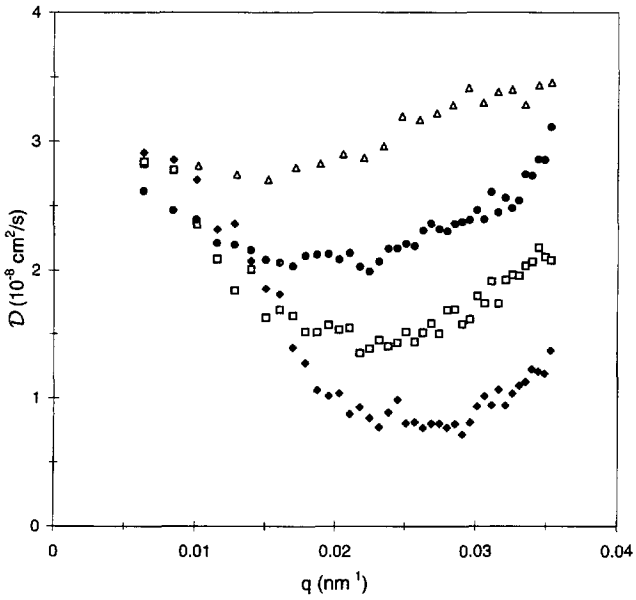

Fig. 7. — Diffusion coefficient $\mathcal{D}$ as a function of the scattering vector q for the same concentrations as in Figure 3 (the symbols have the same meaning). The diffusion coefficient passes through a minimum which is concentration dependent and is the counterpart of the scattered intensity maximum.

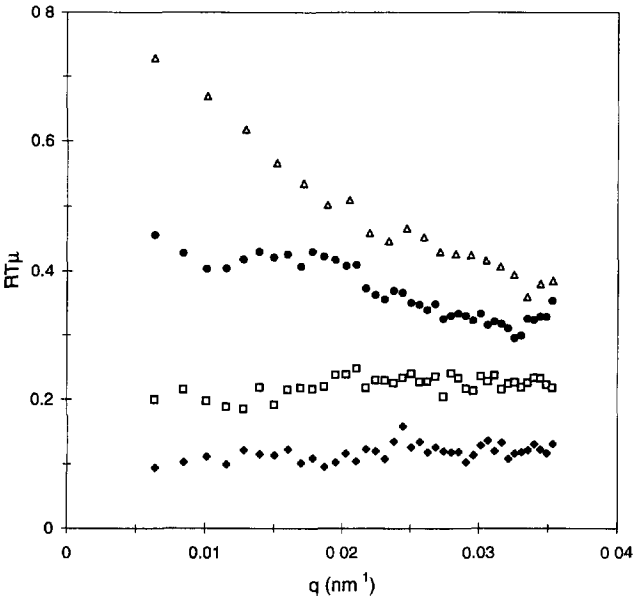

Fig. 8. — Mobility per monomer $RT\mu$ (in erg s mol^{-1}) deduced from the product of the scattered intensity per monomer $I/(KC)$ and the diffusion coefficient $\mathcal{D}$, as a function of the scattering vector q. Symbols have the same meaning as in Figure 3. Monotone curves are found which means that the scattered intensity maximum is well compensated by the diffusion coefficient minimum. The curves tend to merge at high q, but are strongly concentration dependent at low q, because the mobility is influenced by the local (solvent) and macroscopic viscosity, respectively.

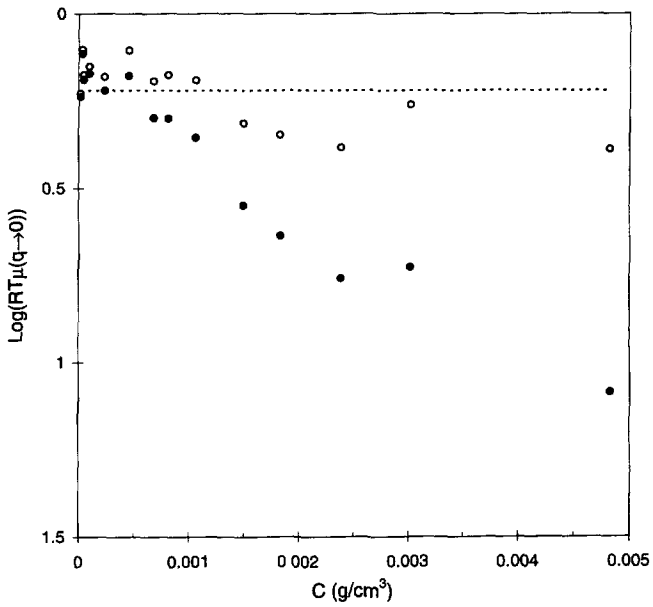

Fig. 9. — Comparison of the concentration dependence of mobility per monomer $RT\mu_{(q\to 0)}$ (full symbols) and the mobility corrected by the macroscopic viscosity $\eta/\eta_0 \times RT\mu_{(q\to 0)}$ (empty symbols). $\mu_{(q\to 0)}$ is the zero scattering vector limit of the mobility per monomer and η/η_0 the ratio of the macroscopic to the solvent viscosity. One can see that the macroscopic viscosity is mainly responsible for the decrease of the monomer mobility as the concentration increases. The dotted line corresponds to the mean value $\eta/\eta_0 \times RT\mu_{(q\to 0)} = 0.6 \pm 0.1$ erg s mol^{-1}

viscosity for the highest concentration ($C = 5 \times 10^{-3}$ g/cm^3).

In Figure 9, the mobility extrapolated to zero scattering vector is plotted as a function of the concentration. For concentrations $C > 4 \times 10^{-4}$ g/cm^3, the mobility decreases by a factor of 10 as the concentration increases by the same factor. If the size of the micelles is independent of the concentration, then the macroscopic viscosity of the solution accounts for the concentration dependence of the zero q mobility (see Eq. (14)). In order to verify this assumption, the ratio of the macroscopic viscosity to the solvent viscosity η/η_0 was measured using an Ubbelohde capillary on quenched samples having different concentrations ($2 \times 10^{-4} < C$ (g/cm^3) $< 6 \times 10^{-3}$). It is found that:

$$\frac{\eta}{\eta_0} = 1.016 + 308 \times C + (326 \times C)^2 \tag{21}$$

leading to an intrinsic viscosity $[\eta] = 308$ cm^3/g, and the Huggins constant $k_H = 1.03$ in good agreement with the value predicted for hard spheres [22]. The product of the intrinsic viscosity and the overlap concentration C^* is equal to $[\eta] \times C^* = 2.15$, in agreement with the value of 5/2 expected from the Einstein relation.

In Figure 9, the zero q mobility multiplied by the ratio η/η_0 is shown to be concentration independent within 10%, in agreement with our expectation:

$$RT\mu_{(q\to 0)}\frac{\eta}{\eta_0} = (0.62 \pm 0.06) \text{ erg s mol}^{-1} \tag{22}$$

This indicates that micelles move in an effective medium the viscosity of which is the macroscopic viscosity, which is increased by the presence of the other micelles [23].

Discussion and Conclusion

The main results presented in this paper concern dilute solution of micelles formed by the association of diblock copolymers in a selective solvent. The different quantities measured are in favor the existence of star like micelles; the results obtained here are similar to those obtained for star polymers [12].

At low concentrations, where interaction between micelles is negligible, the independence of the diffusion coefficient on the scattering vector q, for $qR_H \leq 2.5$, is a direct evidence for a structure having a high internal concentration. However, the fact that only an apparent radius of gyration R_{gapp} can be measured does not allow us to verify directly the increase in size with the association number p. For $p = 20$, the micelle and the unimer have the same apparent radius of gyration ($R_{gapp}/R_{gapp\ unimer} = 1.06$). However, the ratio of the hydrodynamic radii $R_H/R_{H\ unimer} = 3.59$ and the assumption that $R_{H\ unimer} = 0.64 \times R_{g\ unimer}$ for unimer and $R_H = \sqrt{5/3} \times R_g$ for micelles [24], lead to a rough evaluation of $R_g/R_{g\ unimer} = 1.77$. This ratio is expected [9] to be of the order of $p^{0.2} = 20^{0\ 2} = 1.8$. In part 2 of our paper, we will discuss the experimental verification of the relation between size and mass of star like micelles.

From dynamic measurements sensitive to hydrodynamic interactions, it is shown that the micelles behave as hard spheres, justifying *a posteriori* the assumption $R_t = R_H$. The ratio $R_H/R_{gapp} = 1.56$ measured for micelles corresponds to the lower bound of R_t/R_{gapp}, suggesting that the PI blocks are Gaussian rather than stretched.

At higher concentrations, interaction between micelles becomes preponderant, and the static (the dynamic) structure factor presents a maximum (minimum), revealing the high internal concentration of the micelles. The concentration dependence (as well as the amplitude) of this maximum indicates that in this concentration range, micelles form a liquid phase whose distance between first neighbor is 400 nm at $C = 10^{-3}$ g/cm^3. On the other hand, the mobility per monomer which is only sensitive to hydrodynamic interactions is a monotone function of the scattering vector. This quantity allows us to demonstrate that the motion of each micelle is subjected to the macroscopic viscosity.

References

[1] Halperin A., *Macromolecules* **20** (1987) 2943.
[2] Raspaud E., Lairez D., Adam M. and Carton J.-P., *Macromolecules* **27** (1994) 2956.
[3] Adam M., Lairez D., Raspaud E. and Carton J.-P., in preparation.
[4] Cogan K.A., Gast A.P. and Capel M., *Macromolecules* **24** (1991) 6512.
[5] See for example: Tuzar Z. and Kratochvil P., *Surf. Colloid Sci.* **15** (1992) 1 and references therein.
[6] Luzzati S., Adam M. and Delsanti M., *Polymer* **27** (1986) 834; Adam M., Delsanti M., Munch, J.-P. and Durand D., *J. Phys. France* **48** (1987) 1809.
[7] Rabin Y. and Onuki A., *Macromolecules* **23** (1994) 870.
[8] Daoud M. and Cotton J.-P., *J. Phys. France* **43** (1982) 531.
[9] Adam M. and Lairez D., *Fractals* **1** (1993) 149.

[10] Richter D., Farago B., Fetters L.J., Huang J.S. and Even B., *Macromolecules* **23** (1990) 1845.
[11] Witten T.A., Pincus P.A. and Cates M.E., *Europhys. Lett.* **2** (1986) 137.
[12] Adam M., Fetters L.J., Graessley W.W. and Witten T.A., *Macromolecules* **24** (1991) 2434.
[13] Star like polymers crystallize only if the internal concentration (large f and small M_a) is of the order of 1. Then whatever the external concentration, polymers will not interpenetrate each other and behave as colloid as shown in Richter D., Jucknischke O., Willner L., Fetters L.J., Lin M., Huang J.S., Roovers J., Toporowski P. and Zhou L.L., *Polym. Mater. Sci. Eng.* **67** (1992) 425.
[14] Benoit H. and Leng M., *Ind. Plast. Modernes* **12** (1960).
[15] Cotton J.-P. and Benoit H., *J. Phys. France* **36** (1975) 905.
[16] Bushuk W. and Benoit H., *Canadian J. Chem.* **36** (1958) 1616.
[17] de Gennes P.G., Scaling Concepts in Polymer Physics (Cornell University Press, Ithaca, NY, 1979).
[18] Brochard F., *J. Phys. France* **44** (1983) 39.
[19] Oono Y., *J. Chem. Phys.* **79** (1983) 4629.
[20] Grest G.S., Kremer K., Milner S.T. and Witten T.A., *Macromolecules* **22** (1989) 1904.
[21] In fact, for comparison of CAT and DT, the relevent variable for the concentration is the number of chains per unit volume C/M which is also equal to C_{PS}/M_{PS}. In our case, M_{PS} being constant, we take C_{PS} as the variable.
[22] Yamakawa H., Modern theory of polymer solutions (Harper & Row pub., New York, 1971).
[23] Segré P.N., Meeker S.P., Pusey P.N. and Poon W.C.K., *Phys. Rev. Lett.* **75** (1995) 958.
[24] Vagberg L.J.M., Cogan K.A. and Gast A.P., *Macromolecules* **24** (1991) 1670.